Received: 28 January 2022 | Revised: 26 January 2022 | Accepted: 1 February 2022

DOI: 10.1111/ele.14020

ECOLOGY LETTERS cnrs WILEY

METHOD

A novel analytical framework to quantify co-gradient and countergradient variation

Molly A. Albecker | **Geoffrey C. Trussell** | **Katie E. Lotterhos**

Department of Marine and Environmental Sciences, Northeastern University, Boston, Massachusetts, USA

Correspondence
Molly A. Albecker, Department of Biology, Utah State University, Logan, UT, USA.
Email: malbecker@gmail.com

Present address
Molly A. Albecker, Department of Biology, Utah State University, Logan, Utah, USA

Funding information
National Science Foundation, Grant/Award Number: 1764316

Editor: Tim Coulson

Abstract

Spatial covariance between genotypic and environmental influences on phenotypes (Cov_{GE}) can result in the nonrandom distribution of genotypes across environmental gradients and is a potentially important factor driving local adaptation. However, a framework to quantify the magnitude and significance of Cov_{GE} has been lacking. We develop a novel quantitative/analytical approach to estimate and test the significance of Cov_{GE} from reciprocal transplant or common garden experiments, which we validate using simulated data. We demonstrate how power to detect Cov_{GE} changes over a range of experimental designs. We confirm an inverse relationship between gene-by-environment interactions (GxE) and Cov_{GE}, as predicted by first principles, but show how phenotypes can be influenced by both. The metric provides a way to measure how phenotypic plasticity covaries with genetic differentiation and highlights the importance of understanding the dual influences of Cov_{GE} and GxE on phenotypes in studies of local adaptation and species' responses to environmental change.

KEYWORDS
adaptive plasticity, cogradient variation, countergradient variation, covariance between genotype and environment, genetic-by-environment interactions, local adaptation, maladaptive plasticity, nonadaptive plasticity

INTRODUCTION

Phenotypic variation across environmental gradients can yield important insight into understanding current species distributions and predicting the capacity of species to adapt to future environmental change (Gienapp et al., 2008). One source of trait variation is genotype-by-environment interactions (GxE), where genetic and environmental factors interact to affect phenotype (Hereford, 2009; Josephs, 2018). However, GxE interactions do not fully capture genotypic and environmental effects on phenotypes. Covariance can evolve between phenotypic deviations due to genotype (genotypic effects) and those due to environment (environmental effects) across spatial locations (Cov_{GE}). Stated differently, environmental and genotypic effects on the phenotype can covary positively or negatively across spatial locations (Berven et al., 1979; Conover & Schultz, 1995; Falconer & Mackay, 1996; Levins, 1968; Trussell & Etter, 2001). Cov_{GE} indicates that phenotypic responses are contingent on the strength and direction of the association between genotypic and environmental effects. While the importance of GxE in agriculture, human health and adaptive evolution is recognised (Saltz et al., 2018), Cov_{GE} remains an understudied force driving the evolution of phenotypic change across environmental gradients. Nevertheless, research on Cov_{GE} has led to significant insights into our understanding of evolutionary processes across space (Conover et al., 2009; Conover & Schultz, 1995). For instance, Levins discovered Cov_{GE} in montane populations of Drosophila, challenging the prevailing views that phenotypic variation always accompanies genetic variation (Levins, 1968). Spatial Cov_{GE} has also led to insights into how adaptation can evolve without phenotypic clines, the evolution of latitudinal compensation, Bergmann clines, and how evolution can affect ecological patterns (summarised in Table 1).

The classical model describing phenotypic variation (V_p) for quantitative traits shows that both GxE interactions and Cov_{GE} contribute to trait variance:

$$V_P = V_G + V_E + V_{(GxE)} + 2(CoV_{GE}) + V_{error} \quad (1)$$

In this equation, V_G is the underlying genetic variance and V_E is the environmental variance affecting V_P. V_{GxE} is the effect of GxE, Cov_{GE} captures the covariance between genotypic and environmental effects (Conover et al., 2009; Conover & Schultz, 1995; Falconer & Mackay, 1996), and V_{error} is residual variation. The biological interpretation of these variance components depends on the experimental design (reviewed in Tables S1 and S2), but we focus on designs in which multiple genotypes are raised in multiple environments. Cogradient variation is positive Cov_{GE} (CoGV; $Cov_{GE} > 0$) and occurs when the effect of selection on genotype corresponds with the environmental influence on phenotype, maximising phenotypic differences across environments (Figure 1a). Conversely, countergradient variation is negative Cov_{GE} (CnGV; $Cov_{GE} < 0$) and occurs when the genotypic effect on the phenotype opposes the environmental effect, minimising phenotypic differences across environments (Figure 1b).

GxE and Cov_{GE} can be inferred from reciprocal transplant (i.e. raising individuals in their native and 'new' environments) or common garden experiments (i.e. raising individuals from different locations in shared environments) (Merilä & Hendry, 2014), but past syntheses have focused solely on either GxE (Hereford, 2009) or Cov_{GE} (Conover et al., 2009; Conover & Schultz, 1995). However, in the phenotypic realm, the magnitude of Cov_{GE} is inversely related to the magnitude of GxE: Cov_{GE} is maximised when reaction norms are parallel, and GxE is absent. Conversely, GxE is maximised when reaction norms cross in an 'X' pattern, and there is no Cov_{GE}. However, there are intermediate scenarios when phenotypes may be influenced by both Cov_{GE} and GxE. Despite the likelihood of this dual influence in nature, to our knowledge there have been no explorations of the association between Cov_{GE} and GxE. Hence, we continue to have a poor understanding of the relative contributions of GxE and Cov_{GE} to phenotypic variation in nature.

The studies that have identified CoGV or CnGV have been limited to qualitative assessments of visual patterns because there has been no useful quantitative framework to evaluate the magnitude and significance of CovGE (Conover et al., 2009). Falconer (1989) suggested that Cov_{GE} could be measured indirectly using inbred lines and by controlling for non-random aspects of the environment but did not describe how to estimate Cov_{GE} in the presence of GxE interactions or residual variation. Without a method to test whether observed patterns of Cov_{GE} are statistically different from zero, it is difficult to determine the true prevalence and strength of these patterns in driving evolution across environmental gradients in nature.

TABLE 1 Major advancements in ecology and evolution from spatial Cov_{GE}

Study: Subject	How did it or does it influence the field?
(Levins, 1968): countergradient variation in body size with altitude	Levins discovered that genetic variation for body size was partially counteracting the effect of temperature (which was negatively related to size), thereby moderating the change in body size with altitude that would have otherwise been expressed. He referred to this pattern as 'contragradient variation,' which challenged the then widely held assumption that genetic variation, if any, would parallel phenotypic variation
(Conover & Schultz, 1995): countergradient variation	Identified that investigating Cov_{GE} can reveal the environmental and physiological pathways of adaptation, both of which are essential to understand current and future range limits under climate change. Also pointed out that many instances of local adaptation via countergradient variation could be overlooked, due to a long history of evolutionary biologists focusing on clinal phenotypic variation as evidence of strong selection (e.g. Endler, 1977)
(Levinton, 1983): latitudinal compensation	Latitudinal compensation is a pattern of CnGv in which cooler populations exhibit higher growth and metabolic rates than warmer populations (a type of CnGv). This challenges metabolic theory, which predicts that populations residing in warm locations will have higher rates of growth compared to those residing in cool habitats because warming increases the rate of metabolic processes (Brown et al., 2004).
(Blanckenhorn & Demont, 2004): body size clines with latitude	Degree of CnGv in developmental and growth traits gave insights into debates regarding the mechanisms underpinning variation in body size along latitudinal gradients (e.g. Bergmann's rule and exceptions). Specifically, countergradient variation can reconcile paradoxical patterns in development and growth that occur across latitudinal gradients
(Urban et al., 2020): effect of evolution of Cov_{GE} on ecological patterns in space	This review challenges the ecological inference that can be determined from direct relationships of species traits/abundances and ecological gradients due to Cov_{GE}. For instance, evolution can amplify environmental variation (CoGv), and lead to an overestimation of ecological effects of an environmental gradient. Conversely, evolution can dampen ecological patterns across an environmental gradient (CnGv) which may lead to local adaptation evening out fitness across environments and researchers incorrectly concluding that the environment does not influence ecological patterns

Note: CoGV, cogradient variation; CnGV, countergradient variation.

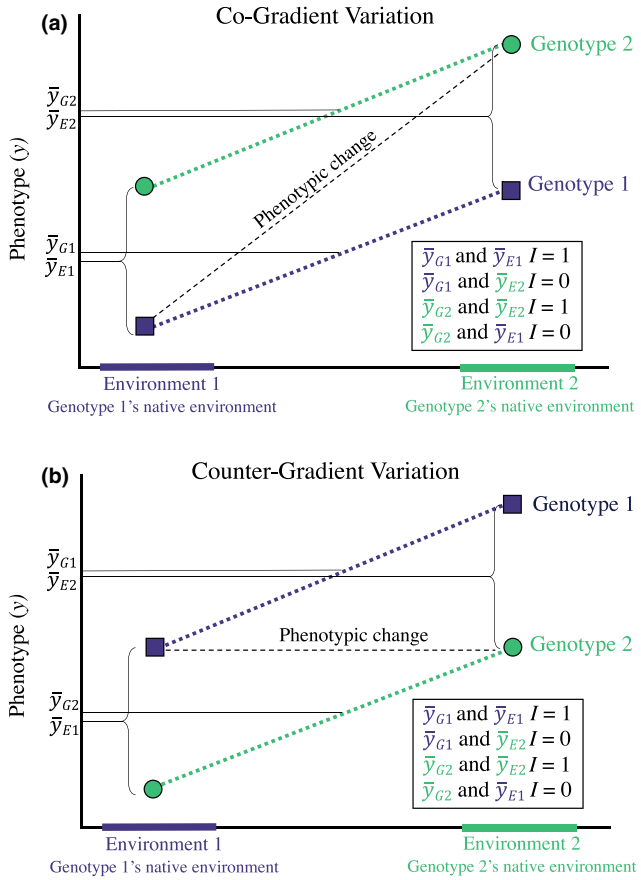

FIGURE 1 In these examples of cogradient variation (a) and countergradient variation (b), we show the sampling estimates that are used to estimate Cov_{GE}. The genetic effect for genotype *i* is the estimated marginal mean phenotype across all environments ($\bar{y}_i$)The environmental effect for environment *j* is the estimated marginal mean phenotype across all genotypes ($\bar{y}_j$) The black dashed line shows the degree of phenotypic change that would be observed in a survey. Genetic effects are then matched with their native environmental effects (in the above example, genotype 1 is native to environment 1, genotype 2 is native to environment 2) and covariance is measured using Equation 2. The inset boxes denote the behavior of the indicator variable (*I*) in Equation 2 for each genotype and environment combination

To better understand the extent to which phenotypes are influenced by Cov_{GE} and GxE across environments, it is critical that we (1) develop a statistical approach that estimates the magnitude and significance of Cov_{GE}, and (2) determine experimental designs that best reveal these patterns. We show that foundational equations in statistics can be used to estimate the magnitude and significance of the effect size of Cov_{GE} for a single phenotype observed across environments and genotypes. We use bootstrap and permutation to determine the uncertainty and significance of Cov_{GE} estimates respectively. This approach (effect size estimation) is fundamentally different from, but complementary to, partitioning phenotypic variance into its different components (as in Equation 1). Thus, our Cov_{GE} estimate is analogous to a correlation and can be compared across datasets with different amounts of residual variation.

To explore the relationship between GxE and Cov_{GE} across datasets with different amounts of residual variation (which is not possible with a traditional ANOVA framework), we also develop a sampling statistic for effect size and significance of GxE. We validate the Cov_{GE} and GxE statistics with simulated and experimental data and show that it is a useful approximation for measuring the magnitude of Cov_{GE} and GxE. We also use simulated data to evaluate the types of experimental designs that are most powerful to disentangle how phenotypes are influenced by Cov_{GE} and/or GxE. Finally, we demonstrate an application on data from two published studies.

METHODS

Spatial Cov_{GE} is an emergent phenomenon in a metapopulation and is not mathematically equivalent to additive genetic covariance (which describes the pleiotropic effect of mutations on multiple traits), nor is it equivalent to covariance between phenotype and environment (which is an evolved property of a genotype that describes the reaction norm) (see Table S3).

Experimental design for spatial Cov_{GE}

Calculating spatial Cov_{GE} requires experimental designs where genotypes sourced from two or more environments are raised in a factorial combination of all sourced environments. We define a *genotype* as a group of interbreeding individuals of the same species that may be connected to other groups via dispersal but maintain some spatial structure or genetic separation (Kawecki & Ebert, 2004). Estimating Cov_{GE} requires phenotypic data that are collected from each genotype within its native environment and the native environments of other genotypes in the experiment. This criterion is met with reciprocal transplant experimental designs, in which multiple individuals of each genotype are collected and transplanted into all locations. Data from common garden experiments, where individuals from different genotypes are grown in the same environmental conditions, can also be used if each genotype's native environment is included as a treatment (See Figure S1 for examples of experimental designs).

Spatial Cov_{GE} magnitude

Cov_{GE} measures the joint variability of genotypic (n_{gen} = number of genotypes) and environmental (n_{env} = number of environments) effects on phenotypes. The estimated value of spatial Cov_{GE} ($\widehat{Cov_{GE}}$) is given as a standardised mean product between corresponding pairs of environmental and genotypic effects sourced from the same native environments. An environmental effect is the difference between the mean phenotype of replicate individuals grown in

environment j (across all genotypes) from the overall mean ($\bar{y}_j - \bar{y}$), while a genotypic effect is the difference between the mean phenotype of replicate individuals from genotype i across all environments ($\bar{y}_i - \bar{y}$; Figure 1):

$$\widehat{Cov_{GE}} = \frac{1}{\sum_{i=1}^{n_{gen}} \sum_{j=1}^{n_{env}} (I_{ij})} \left(\frac{\sum_{i=1}^{n_{gen}} \sum_{j=1}^{n_{env}} (\bar{y}_i - \neg\bar{y})(\bar{y}_j - \neg\bar{y}) I_{ij}}{max\left(s^2_{\bar{y}_i}, s^2_{\bar{y}_j}\right)} \right) \quad (2)$$

where $s^2_{\bar{y}_i}$ is the variance across the average genotypic effects (Methods S1, Equation 2), $s^2_{\bar{y}_j}$ is the variance across the average environmental effects (Methods S1, Equation 3), and I is an indicator variable (see below). To standardise covariance on a scale from −1.0 to 1.0, we divide $\widehat{Cov_{GE}}$ by the larger of the genotypic or environmental variance ($max(s^2_{\bar{y}_i}, s^2_{\bar{y}_j})$); see proof and population equations in Methods S2 and S3). Unlike a traditional correlation (which is standardised by $s^2_{\bar{y}_i} * s^2_{\bar{y}_j}$ and leads to inaccurate estimates of Cov_{GE}), the genotypic and environmental effects are not independent of each other because spatial Cov_{GE} measures the association between genotypic and environmental means. By taking the $max(s^2_{\bar{y}_i}, s^2_{\bar{y}_j})$, we preserve the relationship between the genotypic and environmental effects and bound results between −1 and 1 (Methods S2). We use the indicator variable I_{ij} to only include environmental and genotypic effects in the $\widehat{Cov_{GE}}$ calculation when the genotypic effect is correctly matched with the environmental effect of its native environment. Thus, I_{ij} is 1 when the genotypic and environmental effects of its native environmental are correctly paired and zero otherwise (see inset in Figure 1).

GxE magnitude

To evaluate the relationship between $\widehat{Cov_{GE}}$ and GxE, we needed a sampling estimate of the effect size of GxE that was not influenced by the amount of residual variation in the data (Method S3). We calculated the sampling estimate of the GxE interaction ($\overline{\Delta}_{GxE}$) as the average deviation of the mean of the observed average effects of genotype and environment from that expected phenotype based on the additive effects of genotype and environment, given by:

$$\overline{\Delta}_{GxE} = \frac{1}{(n_{gen})(n_{env})} \sum_{i=1}^{n_{gen}} \sum_{j=1}^{n_{env}} \left| \bar{y}_{ij} - \bar{y}_i - \bar{y}_j + \bar{y} \right| \quad (3)$$

In this equation, $\bar{y}_{ij}$ is the mean phenotype of ith genotype in the jth environment, $\bar{y}_i$ is the mean phenotype for the ith genotype across all environments, $\bar{y}_j$ is the mean phenotype of the jth environment across all genotypes, and $\bar{y}$ is the overall mean phenotype across all genotypes and environments (Queen et al., 2002). As $\overline{\Delta}_{GxE}$ approaches zero, the reaction norms become increasingly parallel (e.g. G + E).

We used estimated marginal means (EMMs) from categorical linear models (e.g. ANOVAs) to generate the $\bar{y}_i$ and $\bar{y}_j$ values to estimate $\widehat{Cov_{GE}}$ and $\overline{\Delta}_{GxE}$ (Equations 2 and 3). Model-fit coefficients reduce bias that may arise from unequal sample sizes within groups (Russell, 2018). To estimate $\bar{y}_i$ and $\bar{y}_j$, we performed an ANOVA that included an interaction between fixed effects of environment and genotype to standardised phenotypic data using function aov() in package 'lme4' (Bates et al., 2014), and extracted EMMs using function emmeans() in package 'emmeans' (Lenth, 2016). We standardised each individual's phenotype by subtracting the overall EMM and dividing by the standard deviation of group means. We define a 'group mean' as the average value among individuals belonging to a specific genotypic and environmental group (*sensu* Whitlock & Schluter, 2009). All analyses and simulations were performed using R (version 3.6.2) (R core team, 2018).

Confidence intervals

We used Monte Carlo methods to calculate confidence intervals (CIs) and conduct hypothesis tests because they make fewer assumptions about the data (Whitlock & Schluter, 2009). We used bootstrapping to determine the level of uncertainty around the $\widehat{Cov_{GE}}$ and $\overline{\Delta}_{GxE}$ estimates. We generated 95% CI by re-sampling with replacement the phenotypic data within each genotype and environment combination 999 times.

Hypothesis testing

We used permutations to test the null hypotheses that $\widehat{Cov_{GE}} = 0$ and $\overline{\Delta}_{GxE} = \overline{\Delta}_{G+E}$ because permutations account for strange distributional properties. We use $\overline{\Delta}_{GxE} = \overline{\Delta}_{G+E}$ as the null expectation to test whether the amount of GxE exceeded that expected based on the additive effects of genotype and environment and to account for the fact that an absolute value cannot overlap zero. $\overline{\Delta}_{GxE}$ is a right-tailed test (H_A: $\overline{\Delta}_{GxE} > \overline{\Delta}_{G+E}$), so the p-value is the proportion of values that were greater than or equal to $\overline{\Delta}_{GxE}$.$\widehat{Cov_{GE}}$ is a two-tailed test (H_A: $\widehat{Cov_{GE}} \neq 0$), so we took the absolute value of $\widehat{Cov_{GE}}$ and the null distribution, making the p-value the proportion of values greater than or equal to $|\widehat{Cov_{GE}}|$. We shuffled standardised phenotypic data 999 times across genotypes and environments without replacement to form null distributions for both $\widehat{Cov_{GE}}$ and $\overline{\Delta}_{G+E}$. P-values were calculated as the proportion of values in the null distribution that were equal or further in the tail(s) than

the sample estimate. *P*-values were compared to $\alpha = 0.05$ to assess significance.

Simulations

To validate the $\widehat{Cov_{GE}}$ and $\overline{\Delta}_{GxE}$ sampling estimates, we created simulations that mimicked experimental data, and provided an array of scenarios to understand how effect size, presence of GxE, total sample size, experimental design, and variability affected $\widehat{Cov_{GE}}$, as well as the ability to detect and measure these patterns. We simulated datasets with total sample sizes (number of environments × number of genotypes × sample size) between 32 and 500 individuals.

For reciprocal transplant data, we simulated genotypic effects that increased linearly at rate γ along an environmental variable (*e*) for genotypes equally spaced from environment $j = [1, 2, \ldots n_{env}]$. We generated unitless phenotypic data based on the equation:

$$phenotype_{ijk} = (i-1)\gamma + \beta e_j + \eta_{ij} + \epsilon_{ijk} \quad (4)$$

In this equation, the phenotype of individual *k* from genotype *i* in environment *j* is given by the genotypic effect (intercept, $(i-1) \times \gamma$), the reaction norm (where e_j is the value of the environment and β is the slope of the reaction norm), an interaction term for genotype *i* in environment *j* (η_{ij}) that describes the deviation of the reaction norm from linearity, and error (ϵ_{ijk}). When $\eta_{ij} = 0$, GxE is absent. When $\gamma = 0$ (i.e. when $V_p = V_E + V_{GxE}$, Equation 1), $\beta = 0$ (i.e. $V_p = V_G + V_{GxE}$, Equation 1), or η_{ij} is large, $\widehat{Cov_{GE}}$ is absent.

Interaction terms (η_{ij}) were drawn from a normal distribution with mean of zero and variance equal to the number of genotypes. Random error (ϵ_{ijk}) was added by sampling from a normal distribution with a mean of zero and standard deviation of either 0.5 (low residual variation) or 1 (high residual variation). Scenarios with no random error (ϵ_{ijk}) were used to assess population parameters (Method S3).

For common garden designs, we adjusted this approach to model designs in which different numbers of genotypes were reared in two common environments (Figure S4c). We generated a single phenotypic reaction norm for each group of genotypes (i.e. genotypes native to the same environment) based on the first terms of Equation 4 (e.g. $(i-1)\gamma + \beta e_j$). Then we generated reaction norm data for individual genotypes by adding the interaction term (η_{ij}) and error (ϵ_{ijk}) to the overall reaction norms.

Evaluation

After simulating phenotypic data, we estimated $\widehat{Cov_{GE}}$ and $\overline{\Delta}_{GxE}$ as well as 95% CI and *P*-values. To assess how confidence intervals and *p*-values performed in assessing significance, we calculated false positive and false negative rates. For $\overline{\Delta}_{GxE}$, we compared error rates to the *F*-test for GxE from an ANOVA.

We assessed power by determining the proportion of times that we correctly rejected the null hypothesis (H_0: $\widehat{Cov_{GE}} = 0$ or $\overline{\Delta}_{GxE} = \overline{\Delta}_{G+E}$) for moderate effect sizes. Moderate values of $|\widehat{Cov_{GE}}|$ and $\overline{\Delta}_{GxE}$ fell between 0.2 and 0.5 in scenarios with high levels of residual error ($\epsilon_{ijk} = 1$). We then determined which experimental designs were most powerful in identifying $\widehat{Cov_{GE}}$ and $\overline{\Delta}_{GxE}$.

Examples from published data

We applied the analytical approach described above to determine the magnitude, certainty, and significance of $\widehat{Cov_{GE}}$ and $\overline{\Delta}_{GxE}$ on phenotypic data from two published studies. We chose these studies because each qualitatively observed countergradient variation patterns, reported the native environments for each genotype, and included each genotype's native environment as a treatment.

The first study, Albecker and McCoy (2019), used a common garden design to investigate the impacts of saltwater exposure on larval frog (*Dryophytes cinerea*) development collected from coastal and inland locations. We analysed 'age at metamorphosis' data, which measured the number of days between egg hatching and metamorphosis. The four coastal and inland populations were separate genotypes that were native to the saltwater or freshwater environment (respectively) (Albecker & McCoy, 2017). We omitted one inland genotype because there were no survivors in the saltwater treatment. Because our approach requires that each genotype's native environment is included as a treatment, we only used data from two environments (freshwater and 6 parts per thousand [ppt] salinity (hereafter called 'saltwater'). Data were provided by the authors.

We applied our methods to a second study that investigated patterns of local adaptation in Red-shouldered soapberry bugs (*Jadera haematoloma*) (Cenzer, 2017). This study used a common garden design to test whether soapberry bugs have become locally adapted to introduced or native host plants. Individuals were offspring (F2 generation) that were either native to *Cardiospermum corindumand* (the native host plant species) collected from three locations (three genotypes), or native to the introduced host plant (*Koelreuteria elegans*) collected from five locations (five genotypes). We accessed the data via datadryad.org (https://doi.org/10.5061/dryad.bn89r) and analysed forewing length data for male and female bugs.

The common garden designs in the above studies are imbalanced in the numbers of genotypes collected from each native environment (Figure S2). This imbalance biases the overall mean ($\overline{y}$) and environmental estimated mean phenotype ($\overline{y}_j$), and therefore biases $\widehat{Cov_{GE}}$. In

Table S4, we describe how we calculated unbiased $\widehat{Cov_{GE}}$ for imbalanced designs.

RESULTS

We simulated 10 replicates of phenotypic data for 3315 unique parameter combinations, which produced $\widehat{Cov_{GE}}$ estimates between −1 (strong countergradient variation) and 1 (strong cogradient variation) (Figure S3). Comparisons two-genotype/two environment scenarios, reciprocal transplant scenarios, and common garden designs revealed how the sampling estimates can be used to compare Cov_{GE} and GxE (Figure S4). The sampling estimates were good estimates of the population parameters (Figure S5).

Error rates for $\widehat{Cov_{GE}}$ based on bootstrapping (i.e., 95% CI do not cross 0) and permutation ($P < \alpha$) for scenarios with higher amounts of residual variation ($\epsilon_{ijk} = 1$) revealed that inference based on permutation had lower false positive rates, whereas inference based on bootstrapped confidence intervals had a nominal increase in false positive rates (Figure 2a,b). Power to detect moderate effect sizes of $\widehat{Cov_{GE}}$ increased with increasing sample size (Figure 3a,b) and was greater for bootstrapped confidence intervals than permutation (dashed green lines above solid green lines in Figure 3). For reciprocal transplant designs with 256 total samples (and higher residual variation), inference for $|\widehat{Cov_{GE}}|$ based on permutation only achieved 80% power at large effect sizes (~0.85)(solid green line; Figure 3c), but common garden designs reached 80% power at moderate effect sizes (~0.4; solid green line; Figure 3d). However, inference based on bootstrap reached 80% power for $|\widehat{Cov_{GE}}|$ at lower effect sizes for both reciprocal transplant (~0.4, dashed green line in Figure 3c) and common garden designs (~0.2, dashed green line in Figure 3d). In summary, bootstrap had more power than permutation to detect differences but also carried a nominal increase in false positive rates, and common garden designs had higher power than reciprocal transplant for similar sample sizes. Higher amounts of variation than simulated here will reduce power.

We also evaluated error rates for $\overline{\Delta}_{GxE}$ based on permutation and ANOVA ($P < \alpha$) using scenarios with higher residual variation. Inference based on bootstrap was found to be unreliable for $\overline{\Delta}_{GxE}$ so we do not include it (Figure S6). Inference based on permutation demonstrated lower false positive rates than ANOVA (Figure 2c and d), but also slightly lower power to detect moderate effect sizes of $\overline{\Delta}_{GxE}$. Nonetheless, both modes of inference are sufficiently powerful to detect moderate (~0.3) to high (>1.0) levels of $\overline{\Delta}_{GxE}$ (purple lines; Figure 3c and d).

An inverse relationship exists between $\widehat{Cov_{GE}}$ and $\overline{\Delta}_{GxE}$ but is characterised by substantial variation because a dataset could have both small but significant $\widehat{Cov_{GE}}$ and $\overline{\Delta}_{GxE}$ (Figure 4a). Another way to understand this inverse relationship is to evaluate how the probability of detecting significant $\widehat{Cov_{GE}}$ decreases with $\overline{\Delta}_{GxE}$. When $\overline{\Delta}_{GxE}$ was low (~0.25), the proportion of significant $\widehat{Cov_{GE}}$ estimates were approximately 80% for both experimental designs (Figure 4b). As $\overline{\Delta}_{GxE}$ grew in magnitude (~0.75), the proportion of significant $\widehat{Cov_{GE}}$ observations dropped to approximately 25%. This inverse relationship was also evident in the variance components (Figure S7).

The $\widehat{Cov_{GE}}$ effect size in Equation 2 provides complementary information to variance components. For example, when $|\widehat{Cov_{GE}}|$ is maximised, equal amounts of non-residual variance are explained by V_G, V_E and V_{CovGE} for the fully factorial reciprocal transplant experiment (Figure S8a). Similarly, intermediate values of $|\widehat{Cov_{GE}}|$ can be driven by higher V_E and lower V_G, or lower V_E and higher V_G (Figure S8b&c).

Applying our method (corrected for imbalanced numbers of genotypes) to the time to metamorphosis data from Albecker & McCoy, 2019 yielded a $\widehat{Cov_{GE}}$ of −0.42 (95% CI −0.49 to −0.32; $p = 0.067$) and a $\overline{\Delta}_{GxE}$ of 0.298 ($p = 0.99$) (Figure 5a). The p-value for Cov_{GE} is slightly above α, but because 95% confidence intervals were not close to zero, we interpreted this $\widehat{Cov_{GE}}$ as significant because permutations have lower power compared to the bootstrapped CI. This study had a total sample size of 187.

Analysis of data on male forewing length phenotype (Figure 5b) from Cenzer (2017) supports the paper's original interpretation ($\widehat{Cov_{GE}} = -0.51$; 95% CI: {−0.78, −0.12}; p-value = 0.009; $\overline{\Delta}_{GxE} = 0.37$; $p = 0.99$) but data for females (Figure 5c), did not reveal significant patterns ($\widehat{Cov_{GE}} = -0.03$, 95% CI: {−0.36, 0.08}; $p = 0.65$; $\overline{\Delta}_{GxE} = 0.27$, p-value = 0.99). This study had a total sample size of 40 for males and 58 for females, which demonstrates that small studies can have sufficient power to detect significant effects depending on the residual variation.

DISCUSSION

Local adaptation can be shaped by both genetic and environmental influences on phenotypic variation but determining their relative contributions to patterns of phenotypic change can be difficult (Endler, 1986; MacColl, 2011). Overcoming this challenge is key because parsing out the relative contributions of plasticity versus genetic evolution in phenotypic variation will enhance our understanding of range limits, patterns of local adaptation and responses to climate change (Boutin & Lane, 2014; Charmantier & Gienapp, 2014; Merilä & Hendry, 2014; Stamp & Hadfield, 2020). The discovery of spatial Cov_{GE} in 1967 had an important influence on views of patterns of phenotypic variation and eco-evolutionary dynamics (Table 1). Thus, a new statistical test that quantifies the strength and

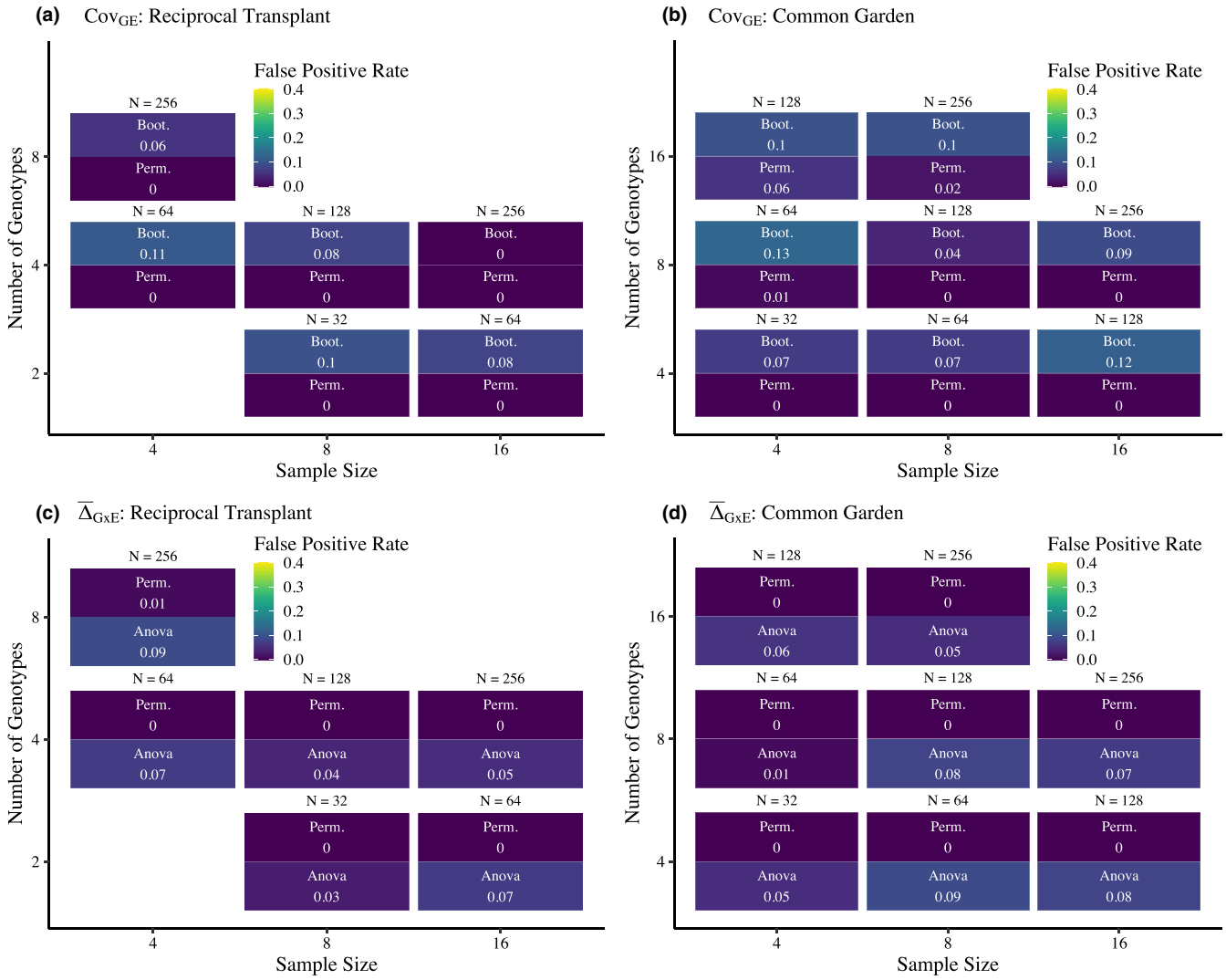

FIGURE 2 Heat maps showing the false positive rates for $\widehat{Cov_{GE}}$ (a, b) and $\overline{\Delta}_{GxE}$ (c, d) according to sample size and the number of genotypes for cases with high residual error. In a and b, tiles show false positive rates according to bootstrapping (upper tile) or permutation (lower tile). In c and d, tiles show false-positive rates according to permutation (upper tile) or ANOVA (lower tile) (Bootstrapping was unreliable for $\overline{\Delta}_{GxE}$, see Figure S6). *N* above each tile set indicates the total sample size (number of genotypes x number of environments x number of samples)

direction of spatial for phenotypic data should accelerate research on the role of Cov$_{GE}$ in eco-evolutionary dynamics.

Spatial Cov$_{GE}$ and GxE give different insights into the processes that drive and maintain local adaptation. Strong spatial Cov$_{GE}$ patterns manifest as near-parallel reaction norms with different intercepts, while strong GxE is revealed by a non-parallel pattern in reaction norms. Since GxE for fitness is a prerequisite for local adaptation (Kawecki & Ebert, 2004), claiming that both give insights to local adaptation may seem paradoxical. The apparent paradox can be resolved by considering that traits can evolve a pattern of spatial Cov$_{GE}$, while fitness evolves a pattern of GxE. For instance, a congeneric pair of northern and southern marine polychaete species (*Ophryotrocha sp.*) demonstrated CnGV in growth rates, but the northern species demonstrated higher mortality in warmer water indicating a GxE relationship in fitness (Levinton, 1983). Although traits showing strong patterns of CoGV and CnGV may not have GxE for *phenotype*, such patterns are reconcilable with local adaptation if the relationship of those traits with fitness differs among populations, resulting in GxE for *fitness*. Because local adaptation is based on fitness and not on traits *sensu stricto*, a GxE for fitness gives insight into adaptation but not plasticity, and does not reveal the traits underlying adaptation (Jong, 2005; Scheiner, 1998).

Significant Cov$_{GE}$ implies that genetic differentiation among populations has evolved in a way that reinforces (CoGv) or opposes (CnGv) the environmental effects on phenotypes. It also implies that different populations have evolved parallel reaction norms to a degree beyond that expected by chance. Although significant

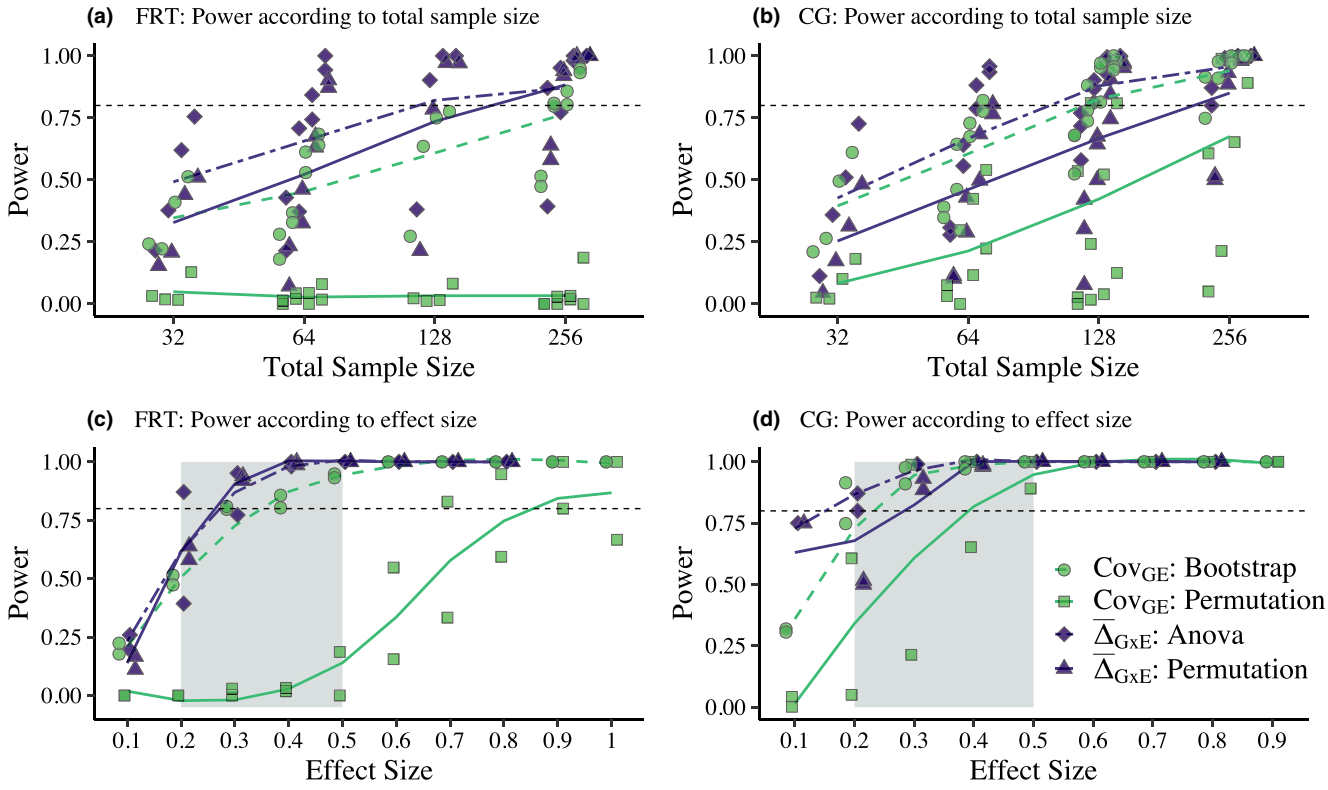

FIGURE 3 Power (defined as 1-ß) to detect $|\widehat{Cov_{GE}}|$ (green) and $\overline{\Delta}_{GxE}$ (purple) for reciprocal transplant (RT: a, c) and common garden (CG: b, d) designs for scenarios with higher amounts of residual variation ($\epsilon_{ijk} = 1$). Dotted black lines indicate 80% power. In each plot, power to detect $|\widehat{Cov_{GE}}|$ is shown for bootstrap methods (green circles; dashed green lines) and permutation methods (green squares; solid green lines). We show power for $\overline{\Delta}_{GxE}$ for ANOVA (purple diamonds; dot-dashed purple lines) and when using permutation methods (purple triangle; solid purple lines). Bootstrap for $\overline{\Delta}_{GxE}$ is not shown because it is unreliable for $\overline{\Delta}_{GxE}$ (Figure S6). Panels A and B are filtered to show the power to detect moderate effect sizes (between 0.2 and 0.5) of $|\widehat{Cov_{GE}}|$ and $\overline{\Delta}_{GxE}$ according to total sample size, which corresponds with the shaded area in panels c and d. Total sample size is the number of genotypes x number of environments x number of samples. Panels c and d are filtered to show power to detect $|\widehat{Cov_{GE}}|$ and $\overline{\Delta}_{GxE}$ according to effect size when 256 total samples are measured

Cov_{GE} does not necessarily imply local adaptation for fitness, many classical examples of Cov_{GE} (Berven et al., 1979; Conover & Present, 1990) are from locally adapted species, and recognition of Cov_{GE} has led to a deeper understanding of local adaptation in these systems. Similarly, significant Cov_{GE} does not necessarily imply that the reaction norm is influenced solely by organismal processes, because both abiotic and biotic processes influence the reaction norm (Falconer, 1989; Havird et al., 2020).

CoGV implies that selective processes determining the phenotypic optima across locations act in the same direction as the processes generating the reaction norm and is thus a type of adaptive plasticity (Conover, 1998). By contrast, CnGV implies that the selective processes determining phenotypic optima across locations oppose the processes generating the reaction norm. Hence CnGV represents a type of nonadaptive (or maladaptive) plasticity. In both cases, the metric provides a way to measure how phenotypic plasticity covaries with genetic differentiation across spatial gradients, while potentially illuminating candidate physiological pathways that underpin Cov_{GE}. For example, when exposed to sublethal saltwater concentrations, freshwater organisms expend energy processing osmotic stress that would otherwise be used for growth or development. In the amphibian dataset, significant CnGV in amphibian larval period illuminated genetic differentiation in the physiological pathways that counter the growth/development costs that are otherwise induced by exposure to saltwater (Albecker & McCoy, 2019). In the soapberry bug study, it was assumed that local adaptation to different host plants had occurred, but phenotypic differentiation expected with divergence was lacking. Identifying significant CnGV confirmed that genetic differentiation had evolved and provided an explanation for the lack of apparent phenotypic differentiation (Cenzer, 2017). Although this study focused on beak length, identifying CnGV in male wing length suggests that selection has acted upon male flying or dispersal ability, which could stimulate new research into sexual differences in this species.

Spatial Cov_{GE} may play an important role with respect to the ecological impacts of climate change (Arietta & Skelly, 2021; Gienapp et al., 2008; Merilä, 2012). Theoretical studies exploring the role of adaptation and plasticity in population responses to climate change typically model temporally fluctuating environments

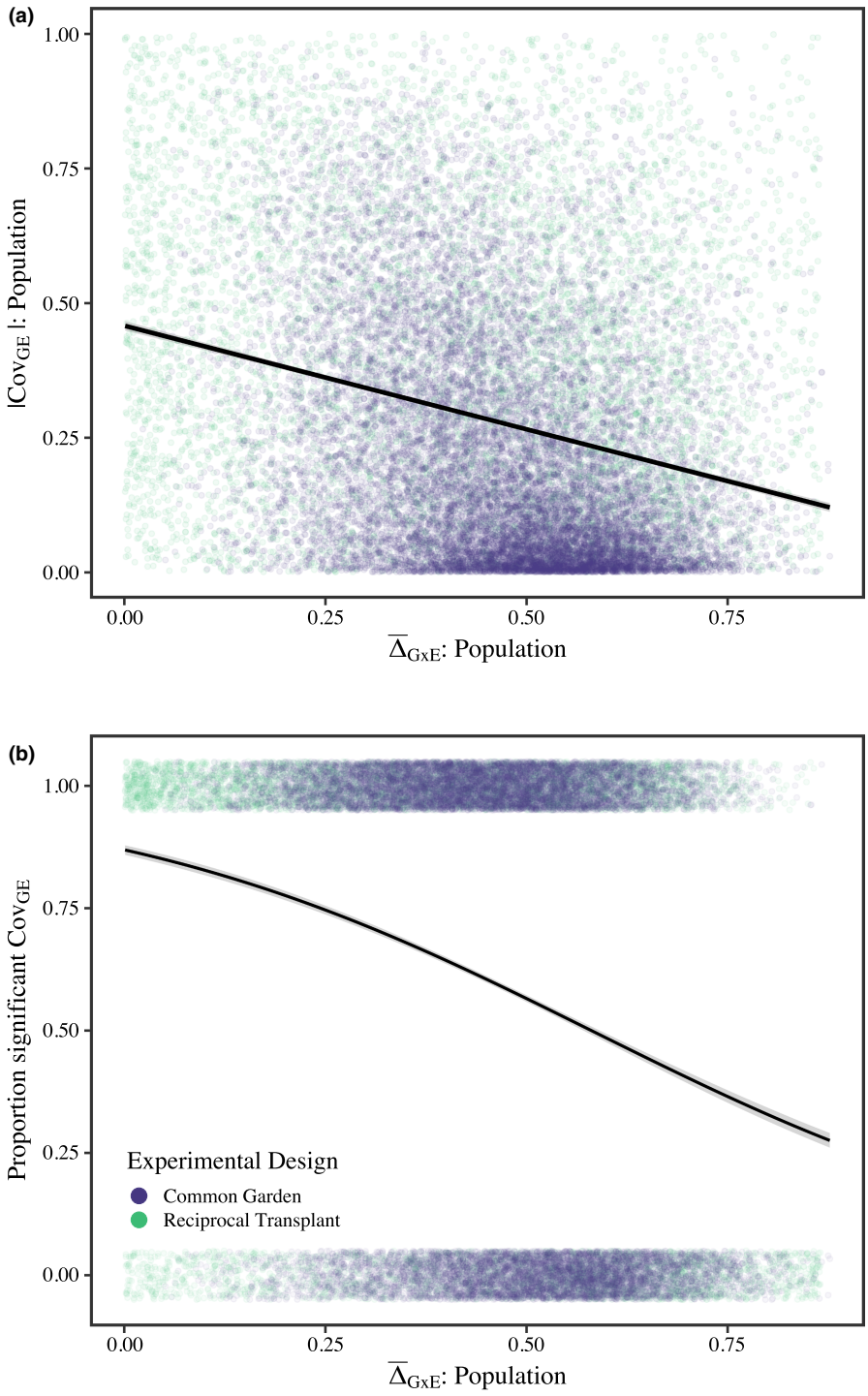

FIGURE 4 Relationships between Cov_{GE} and $\overline{\Delta}_{\text{GxE}}$. Data in these plots are filtered to show just instances of significant $\widehat{Cov_{GE}}$ or $\overline{\Delta}_{\text{GxE}}$, with false positives removed. Panel a shows the inverse relationship between the magnitudes of $|\widehat{Cov_{GE}}|$ and $\overline{\Delta}_{\text{GxE}}$ for common garden (purple points) and reciprocal transplant (green points) experimental designs. Panel b shows that the proportion of significant $\widehat{Cov_{GE}}$ values decrease as $\overline{\Delta}_{\text{GxE}}$ increases. In panel b, data has been filtered to remove false positives, and points are slightly offset along the y-axis for visualization

without including a spatial component (Ashander et al., 2016; Chevin & Hoffmann, 2017; Chevin et al., 2010; Coulson et al., 2017, 2021; Lande, 2009; Scheiner et al., 2017, 2019), and thus do not capture the potential influence of spatial Cov_{GE}. Some of these studies modeled intrinsic properties of the genotype-phenotype map as covariance in pleiotropic effects on multiple traits (Coulson et al., 2017, 2021; Via et al., 1995), but how genetic (co)variance influences the pattern of spatial Cov_{GE} in a metapopulation, and thus metapopulation's responses to climate change, has not been rigorously addressed by theory and remains an important area of

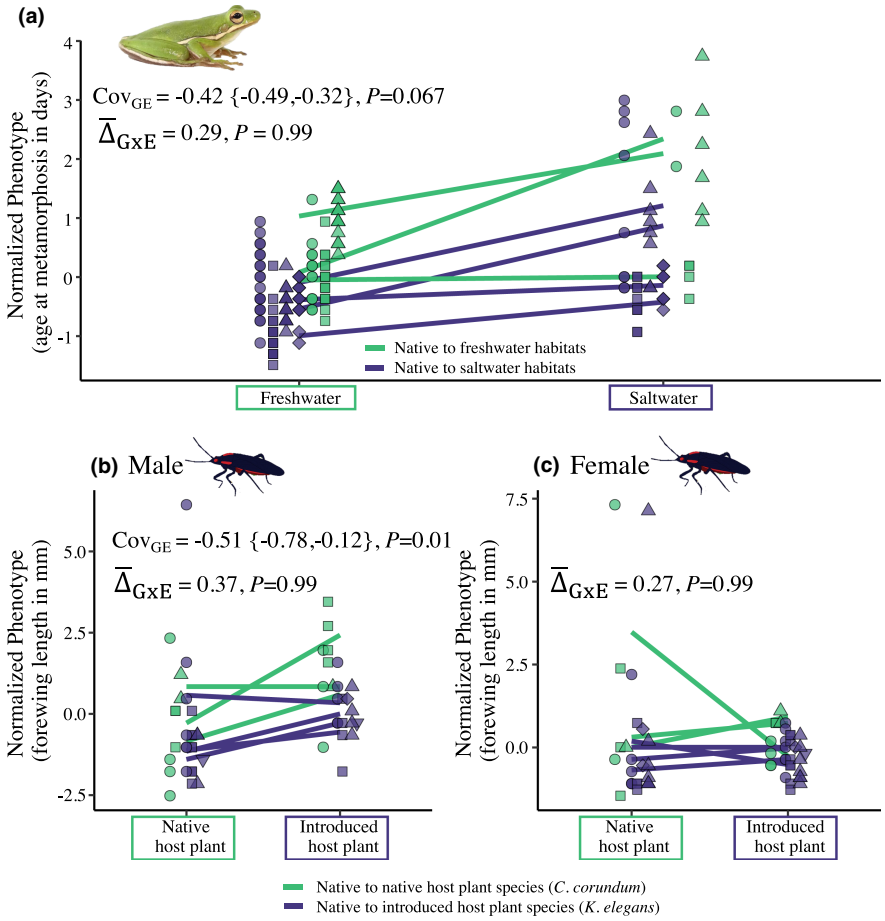

FIGURE 5 Phenotypic reaction norms for the data collected from two published studies (Cenzer, 2017; Albecker & McCoy, 2019) analysed for $\widehat{Cov_{GE}}$ and $\overline{\Delta}_{GxE}$. Reaction norms and points are coloured to correspond to each genotype's native environment overlaid on individual data points (point shapes to denote separate genotypes). Panel a shows normalised age at metamorphosis data from green tree frog populations (*Dryophytes cinereus*) native to freshwater and saltwater habitats that were exposed to freshwater or saltwater treatments (Albecker & McCoy, 2019). Age at metamorphosis demonstrates countergradient variation ($\widehat{Cov_{GE}} = -0.42$ (95% Confidence Interval: {−0.49, −0.32}; $p = 0.067$) with non-significant $\overline{\Delta}_{GxE}$ ($\overline{\Delta}_{GxE} = 0.29$, $p = 0.99$). Panels B and C show normalised forewing length (mm) data from male (b) and female (c) Red-shouldered soapberry bugs (*Jadera haematoloma*) according to data from (Cenzer, 2017). Male soapberry bug wing length (b) is countergradient ($\widehat{Cov_{GE}} = -0.41$, 95% CI: {−0.57, −0.18}; $p = 0.009$), with no significant $\overline{\Delta}_{GxE}$ ($\overline{\Delta}_{GxE} = 0.37$, $p = 0.99$). Contrastingly, female soapberry bugs wing lengths (c) show no gradient patterns ($\widehat{Cov_{GE}} = -0.03$, 95% CI: {−0.36, 0.08}; $p = 0.65$) with non-significant $\overline{\Delta}_{GxE}$ ($\overline{\Delta}_{GxE} = 0.27$, $p = 0.99$). Panels B and C only show 4 introduced plant host reaction norms (out of the expected five) because one genotype only had one sample

future research. The metric provided here can now be combined with more traditional metrics (reviewed in Table S3) to address this gap.

There is an urgent need to better understand how genetic and environmental factors affect responses to novel or changing environments. Because the magnitude and direction of spatial Cov_{GE} will likely affect responses to climate change, incorporation of measurements of spatial Cov_{GE} will enhance our capacity to develop more robust predictions. For example, colder populations are predicted to be maladapted to a warmer climate and vulnerable to climate change (Lotterhos et al., 2021; Sharma et al., 2011). Yet this may not hold under countergradient variation scenarios if the traits under selection in colder environments continue to be adaptive in warmer environments. However, as highlighted by the marine polychaeta example, populations evolved to local optima that did not yield universally higher fitness across environments (Levinton, 1983), which should temper optimistic predictions and stimulate research that applies the metric to understand how spatial Cov_{GE} will affect climate change outcomes.

If spatial Cov_{GE} can mitigate population decline, there are likely ecological consequences for populations exhibiting spatial Cov_{GE} in changing environments. As demonstrated by many taxa (e.g. Arendt & Wilson, 1999; Berven et al., 1979; Carroll et al., 2001; Trussell, 2000; Villeneuve et al., 2021), colder temperatures and shorter growing seasons can induce the evolution of faster growth rates (CnGV), with consequences for life history traits such as size and age at maturity, fecundity,

and developmental rates. Moreover, rapid growth under warmer temperatures may be associated with increased foraging rates and therefore stronger species interactions with implications for community dynamics (Miller et al., 2014; Trussell et al., 2003; Trussell & Schmitz, 2012) and ecosystems (Schmitz et al., 2008, 2010). For example, the indirect effects of predators on lower trophic levels can be shaped by the environmental impacts on the foraging rates of species in the middle of food chains (Schmitz & Trussell, 2016; Trussell & Schmitz, 2012). Many mid-trophic-level species are ectotherms that are sensitive to temperature, and Cov_{GE} may influence how foraging rates respond to warming. Because food web diversity is dominated by middle trophic levels (60% of the total species; Williams & Martinez, 2000), spatial Cov_{GE} in foraging traits within these trophic levels may strongly influence ecosystems. Thus, an important area of future research will be to determine how spatial Cov_{GE} and environmental change interact to influence species traits, species interactions and their cascading effects on ecosystems.

CONCLUSIONS

Cov_{GE} has advanced our understanding of range limits, latitudinal compensation, Bergmann's rule, the effects of evolution on ecological patterns in space, and how local adaptation can evolve in the absence of phenotypic clines. In the past, Cov_{GE} has been inferred from visual patterns, but with the new metric, we can now study Cov_{GE} with an increased level of statistical rigor to advance knowledge of how Cov_{GE} evolves, the ecological consequences of Cov_{GE}, the relative influence of Cov_{GE} vs. GxE on eco-evolutionary dynamics, and how patterns of spatial Cov_{GE} alter metapopulation responses to climate change.

ACKNOWLEDGEMENTS

The authors thank three anonymous reviewers, David Conover, and the editor for their thoughtful feedback that improved the quality of this manuscript. The authors also thank the Lotterhos lab (Aki Laruson, Alan Downey-Wall, Sara Schaal, F. Dylan Titmuss, and Thais Bittar) for helpful feedback and edits. This work was funded through an NSF grant awarded to KEL and GCT (NSF-OCE #1764316).

AUTHOR CONTRIBUTIONS

MAA, GCT, and KEL conceived the idea. MAA and KEL developed the approach. MAA performed simulations and led the writing of the manuscript. All authors verified and discussed findings and contributed to the writing of the final manuscript. KEL and GCT obtained funding. KEL conceptualised the metrics and administered the project.

PEER REVIEW

The peer review history for this article is available at https://publons.com/publon/10.1111/ele.14020.

DATA AVAILABILITY STATEMENT

All data and code, including a tutorial for implementing this approach with real data, is available online at https://github.com/RCN-ECS/CnGV. Upon acceptance of the manuscript, we will archive the code and simulated datasets on Dryad https://zenodo.org/badge/latestdoi/189079692.

ORCID

Molly A. Albecker https://orcid.org/0000-0002-5121-8101
Katie E. Lotterhos https://orcid.org/0000-0001-7529-2771

REFERENCES

Albecker, M.A. & McCoy, M.W. (2017) Adaptive responses to salinity stress across multiple life stages in anuran amphibians. *Frontiers in Zoology*, 14, 40.

Albecker, M.A. & McCoy, M.W. (2019) Local adaptation for enhanced salt tolerance reduces non-adaptive plasticity caused by osmotic stress. *Evolution*, 73(9), 1941–1957.

Arendt, J.D. & Wilson, D.S. (1999) Countergradient selection for rapid growth in pumpkinseed sunfish: disentangling ecological and evolutionary effects. *Ecology*, 80, 2793–2798.

Arietta, A.Z.A. & Skelly, D.K. (2021) Rapid microgeographic evolution in response to climate change. *Evolution*, 75, 2930–2943.

Ashander, J., Chevin, L.-M. & Baskett, M.L. (2016) Predicting evolutionary rescue via evolving plasticity in stochastic environments. *Proceedings of the Royal Society B: Biological Sciences*, 283(1839), 20161690.

Bates, D., Maechler, M., Bolker, B. & Walker, S. (2014). R package. lme4: linear mixed-effects models using Eigen and S4.

Berven, K.A., Gill, D.E. & Smith-Gill, S.J. (1979) Countergradient selection in the Green Frog, Rana clamitans. *Evolution*, 33, 609–623.

Blanckenhorn, W.U. & Demont, M. (2004) Bergmann and converse Bergmann latitudinal clines in arthropods: two ends of a continuum? *Integrative and Comparative Biology*, 44, 413–424.

Boutin, S. & Lane, J.E. (2014) Climate change and mammals: evolutionary versus plastic responses. *Evolutionary Applications*, 7, 29–41.

Brown, J.H., Gillooly, J.F., Allen, A.P., Savage, V.M. & West, G.B. (2004) Toward a metabolic theory of ecology. *Ecology*, 85, 1771–1789.

Carroll, S.P., Dingle, H., Famula, T.R. & Fox, C.W. (2001) Genetic architecture of adaptive differentiation in evolving host races of the soapberry bug, *Jadera haematoloma*. *Genetica*, 112–113, 257–272.

Cenzer, M.L. (2017) Maladaptive plasticity masks the effects of natural selection in the red-shouldered soapberry bug. *The American Naturalist*, 190(4), 521–533.

Charmantier, A. & Gienapp, P. (2014) Climate change and timing of avian breeding and migration: evolutionary versus plastic changes. *Evolutionary Applications*, 7, 15–28.

Chevin, L.-M. & Hoffmann, A.A. (2017) Evolution of phenotypic plasticity in extreme environments. *Philosophical Transactions of the Royal Society B: Biological Sciences*, 372(1723), 20160138.

Chevin, L.-M., Lande, R. & Mace, G.M. (2010) Adaptation, plasticity, and extinction in a changing environment: towards a predictive theory. *PLoS Biology*, 8,e1000357.

Conover, D.O. (1998) Local adaptation in marine fishes: evidence and implications for stock enhancement. *Bulletin of Marine Science*, 62(2), 477–493.

Conover, D.O., Duffy, T.A. & Hice, L.A. (2009) The covariance between genetic and environmental influences across ecological gradients. *Annals of the New York Academy of Sciences*, 1168, 100–129.

Conover, D.O. & Present, T.M.C. (1990) Countergradient variation in growth rate: compensation for length of the growing season among Atlantic silversides from different latitudes. *Oecologia*, 83, 316–324.

Conover, D.O. & Schultz, E.T. (1995) Phenotypic similarity and the evolutionary significance of countergradient variation. *Trends in Ecology and Evolution*, 10, 248–252.

Coulson, T., Kendall, B.E., Barthold, J., Plard, F., Schindler, S., Ozgul, A. et al. (2017) Modeling adaptive and nonadaptive responses of populations to environmental change. *American Naturalist*, 190, 313–336.

Coulson, T., Potter, T. & Felmy, A. (2021) Predicting evolution over multiple generations in deteriorating environments using evolutionarily explicit Integral Projection Models. *Evolutionary Applications*, 14, 2490–2501.

de Jong, G. (2005) Evolution of phenotypic plasticity: patterns of plasticity and the emergence of ecotypes. *New Phytologist*, 166, 101–117.

Endler, J.A. (1977) *Geographic variation, speciation, and clines*. Princeton, NJ: Princeton University Press.

Endler, J.A. (1986) *Natural selection in the wild*. Princeton: Princeton University Press.

Falconer, D.S. (1989) *Introduction to quantitative genetics*. New York: Longman.

Falconer, D.S. & Mackay, T.F.C. (1996) *Introduction to quantitative genetics*. Essex, UK: Longman Group.

Gienapp, P., Teplitsky, C., Alho, J.S., Mills, J.A. & Merilä, J. (2008) Climate change and evolution: disentangling environmental and genetic responses. *Molecular Ecology*, 17, 167–178.

Havird, J.C., Neuwald, J.L., Shah, A.A., Mauro, A., Marshall, C.A. & Ghalambor, C.K. (2020) Distinguishing between active plasticity due to thermal acclimation and passive plasticity due to Q 10 effects: why methodology matters. *Functional Ecology*, 34, 1015–1028.

Hereford, J. (2009) A quantitative survey of local adaptation and fitness trade-offs. *The American Naturalist*, 173, 579–588.

Josephs, E.B. (2018) Determining the evolutionary forces shapingG × E. *New Phytologist*, 219, 31–36.

Kawecki, T.J. & Ebert, D. (2004) Conceptual issues in local adaptation. *Ecology Letters*, 7, 1225–1241.

Lande, R. (2009) Adaptation to an extraordinary environment by evolution of phenotypic plasticity and genetic assimilation. *Journal of Evolutionary Biology*, 22, 1435–1446.

Lenth, R.V. (2016) Least-squares means: The R package lsmeans. *Journal of Statistical Software*, 69, 1–33.

Levins, R. (1968) *Evolution in changing environments: some theoretical explorations*. Princeton: Princeton University Press.

Levinton, J.S. (1983) The latitudinal compensation hypothesis: growth data and a model of latitudinal growth differentiation based upon energy budgets. Interspecific comparison of Ophryotrocha (Polychaeta: Dorvilleidae). *Biological Bulletin*, 165, 686–698.

Lotterhos, K.E., Láruson, Á.J. & Jiang, L.Q. (2021) Novel and disappearing climates in the global surface ocean from 1800 to 2100. *Scientific Reports*, 11(1), 1–16.

MacColl, A.D.C. (2011) The ecological causes of evolution. *Trends in Ecology & Evolution*, 26, 514–522.

Merilä, J. (2012) Evolution in response to climate change: in pursuit of the missing evidence. *BioEssays*, 34, 811–818.

Merilä, J. & Hendry, A.P. (2014) Climate change, adaptation, and phenotypic plasticity: the problem and the evidence. *Evolutionary Applications*, 7, 1–14.

Miller, L.P., Matassa, C.M. & Trussell, G.C. (2014) Climate change enhances the negative effects of predation risk on an intermediate consumer. *Global Change Biology*, 20, 3834–3844.

Queen, J.P., Quinn G.P. & Keough, M.J. (2002) *Experimental design and data analysis for biologists*. Cambridge: Cambridge University Press.

R Core Team. (2018). R: A language and environment for statistical computing; 2015.

Russell, L. (2018) Emmeans: estimated marginal means, aka least-squares means. R Package Version, 1.

Saltz, J.B., Bell, A.M., Flint, J., Gomulkiewicz, R., Hughes, K.A. & Keagy, J. (2018) Why does the magnitude of genotype-by-environment interaction vary? *Ecology and Evolution*, 8(12), 6342–6353.

Scheiner, S.M. (1998) The genetics of phenotypic plasticity. VII. Evolution in a spatially-structured environment. *Journal of Evolutionary Biology*, 11, 303–320.

Scheiner, S.M., Barfield, M. & Holt, R.D. (2017) The genetics of phenotypic plasticity. XV. Genetic assimilation, the Baldwin effect, and evolutionary rescue. *Ecology and Evolution*, 7, 8788–8803.

Scheiner, S.M., Barfield, M. & Holt, R.D. (2019) The genetics of phenotypic plasticity. XVII. Response to climate change. *Evolutionary Applications*, 17, 771.

Schmitz, O.J., Grabowski, J.H., Peckarsky, B.L., Preisser, E.L., Trussell, G.C. & Vonesh, J.R. (2008) From individuals to ecosystem function: toward an integration of evolutionary and ecosystem ecology. *Ecology*, 89, 2436–2445.

Schmitz, O.J., Hawlena, D. & Trussell, G.C. (2010) Predator control of ecosystem nutrient dynamics. *Ecology Letters*, 13, 1199–1209.

Schmitz, O.J. & Trussell, G.C. (2016) Multiple stressors, state-dependence and predation risk—foraging trade-offs: toward a modern concept of trait-mediated indirect effects in communities and ecosystems. *Current Opinion in Behavioral Sciences*, 12, 6–11.

Sharma, S., Vander Zanden, M.J., Magnuson, J.J. & Lyons, J. (2011) Comparing climate change and species invasions as drivers of coldwater fish population extirpations. *PLoS One*, 6(8), e22906.

Stamp, M.A. & Hadfield, J.D. (2020) The relative importance of plasticity versus genetic differentiation in explaining between population differences; a meta-analysis. *Ecology Letters*, 23, 1432–1441.

Trussell, G.C. (2000) Phenotypic clines, plasticity, and morphological trade-offs in an intertidal snail. *Evolution*, 54, 151–166.

Trussell, G.C. & Etter, R.J. (2001) Integrating genetic and environmental forces that shape the evolution of geographic variation in a marine snail. *Genetica*, 112–113, 321–337.

Trussell, G.C., Ewanchuk, P.J. & Bertness, M.D. (2003) Trait-mediated effects in rocky intertidal food chains: predator risk cues alter prey feeding rates. *Ecology*, 84, 629–640.

Trussell, G.C. & Schmitz, O.J. (2012) Species functional traits, trophic control and the ecosystem consequences of adaptive foraging in the middle of food chains. In Ohgushi, T, Schmitz, O.J. & Holt, R.D. (Eds.) *Trait-mediated indirect interactions: ecological and evolutionary perspectives*, Cambridge: Cambridge University Press, pp. 324–338.

Urban, M.C., Strauss, S.Y., Pelletier, F., Palkovacs, E.P., Leibold, M.A., Hendry, A.P. et al. (2020) Evolutionary origins for ecological patterns in space. *Proceedings of the National Academy of Sciences of the United States of America*, 117, 17482–17490.

Via, S., Gomulkiewicz, R., De Jong, G., Scheiner, S.M., Schlichting, C.D. & Van Tienderen, P.H. (1995) Adaptive phenotypic plasticity: consensus and controversy. *Trends in Ecology & Evolution*, 10(5), 212–217.

Villeneuve, A.R., Komoroske, L.M. & Cheng, B.S. (2021) Environment and phenology shape local adaptation in thermal performance. *Proceedings of the Royal Society B: Biological Sciences*, 288, 20210741.

Whitlock, M.C. & Schluter, D. (2009) *The analysis of biological data*. Greenwood Village: Roberts and Company Publishers.

Williams, R.J. & Martinez, N.D. (2000) Simple rules yield complex food webs. *Nature*, 404, 180–183.

SUPPORTING INFORMATION

Additional supporting information may be found in the online version of the article at the publisher's website.

How to cite this article: Albecker, M.A., Trussell, G.C. & Lotterhos, K.E. (2022) A novel analytical framework to quantify co-gradient and countergradient variation. *Ecology Letters*, 25, 1521–1533. Available from: https://doi.org/10.1111/ele.14020